Structure and dynamical intra-molecular heterogeneity of star polymer melts above glass transition temperature

Alexandros Chremos' , Emmanouil Glynos, and Peter F. Green

Citation: The Journal of Chemical Physics **142**, 044901 (2015); doi: 10.1063/1.4906085
View online: http://dx.doi.org/10.1063/1.4906085
View Table of Contents: http://aip.scitation.org/toc/jcp/142/4
Published by the American Institute of Physics

Structure and dynamical intra-molecular heterogeneity of star polymer melts above glass transition temperature

Alexandros Chremos,[1,a)] Emmanouil Glynos,[2] and Peter F. Green[2]
[1]*Department of Chemical Engineering, Centre for Process Systems Engineering, Imperial College London, South Kensington Campus, London SW7 2AZ, United Kingdom*
[2]*Department of Materials Science and Engineering, University of Michigan, Ann Arbor, Michigan 48109, USA*

(Received 5 December 2014; accepted 5 January 2015; published online 23 January 2015)

Structural and dynamical properties of star melts have been investigated with molecular dynamics simulations of a bead-spring model. Star polymers are known to be heterogeneous, but a systematic simulation study of their properties in melt conditions near the glass transition temperature was lacking. To probe their properties, we have expanded from linear to star polymers the applicability of Dobkowski's chain-length dependence correlation function [Z. Dobkowski, Eur. Polym. J. **18**, 563 (1982)]. The density and the isokinetic temperature, based on the canonical definition of the laboratory glass-transition, can be described well by the correlation function and a subtle behavior manifests as the architecture becomes more complex. For linear polymer chains and low functionality star polymers, we find that an increase of the arm length would result in an increase of the density and the isokinetic temperature, but high functionality star polymers have the opposite behavior. The effect between low and high functionalities is more pronounced for short arm lengths. Complementary results such as the specific volume and number of neighbors in contact provide further insights on the subtle relation between structure and dynamics. The findings would be valuable to polymer, colloidal, and nanocomposites fields for the design of materials in absence of solution with the desired properties. © *2015 AIP Publishing LLC.* [http://dx.doi.org/10.1063/1.4906085]

I. INTRODUCTION

The physical properties of polymeric materials are of a paramount importance both from the fundamental perspective and for their various applications.[1] Rouse dynamics and reptation are the main dynamical mechanisms for understanding the dynamical behavior of linear polymer chains in melt conditions.[2,3] However, star polymers representing the simplest case of branched polymers, where f linear polymer chains are grafted onto the surface of a core particle, relax via an arm fluctuation mechanism, which is different from the reptative motion of linear chains.[4] The quantitative description of arm relaxation is due to Milner and McLeish,[5,6] who combined a tube model with the idea of dynamic tube dilation and effectively introducing the key concept of a hierarchy of motions. In other words, entanglements belonging to topologically different parts of the molecular structure relax in a sequence, the outer molecular parts, i.e., the free ends, relax first while the innermost ones last. A distribution of time scales has been shown experimentally for star polymer melts[7] and to a smaller extent in linear chain melts.[8] Nevertheless, the theories for star polymers focus on arms with large molecular weight and the volume fraction of the core particle is negligible. For star polymer with short arms, less attention has been placed.[9] We briefly outline the progress towards understanding these systems and current challenges.

Star polymers in solution to a large extend rely on the Daoud-Cotton model[10] (for reviews, see Refs. 11–15), where a star polymer in solution is represented through scaling arguments by concentric shells of blobs and three regions are identified: the core, the swollen, and unswollen regions. The significance of these regimes is reflected on: (a) for the core regime, the radial monomer distribution is constant, (b) for the unswollen regime, the interactions resemble θ-solvent conditions, and (c) for the swollen region, the spatial dilation provides enough room for excluded volumes to enforce self-avoiding behavior. Based on this model, Likos *et al.*[16] mapped a star polymer onto a single spherical blob, where each blob interacts with pairwise additive interactions. This implicit model was used to explore the phase diagram of star polymer solutions,[17] where a number of crystal structures were found including face-centered cubic, body-centered cubic, and diamond lattices. The key molecular parameter is f, where an increase of f leads to an enhancement of the repulsions between the star polymers.[16] This enhancement of repulsions has made star polymers a bridge between linear polymers and colloids and star polymers are often described as soft colloids.[9,16–23] Although star polymers in a melt can be considered equivalent to an ideal solvent, it has been argued recently by Yu and Koch[24] that star-like macromolecules in the absence of solvent, i.e., melt conditions, may not be sufficiently described by pairwise additive potentials, because the arms would stretch to seek and fill the interstitial voids and thus deforming the molecules. This entropic in origin penalty would be dominant to star polymers with short arms, since entropic effects are more pronounced for short chains.[25] Thus, an explicit model that takes into account space-feeling effects is required to capture the subtle structural and dynamical behavior of a star

a)Electronic mail: achremos@imperial.ac.uk

polymer melt and its dependence on molecular architecture, which are necessary "ingredients" for the design of materials with the desired properties.

The role of molecular architecture plays a significant role in the system properties. For example, the branch point affects the "packing" of not only the polymer segments but also the entire macromolecule, particularly for sufficiently large f. Moreover, the asymmetry in the relaxations between the segments near the free-ends, and those near the branch point of the star polymer signify a molecular intra-molecular heterogeneous behavior. Thus, a key question is how the molecular intra-molecular heterogeneous behavior affects the properties of the polymeric system. Properties like the isokinetic temperature, characteristic ratio, and monomer density are shown[8] to have the same functional chain-length dependence, e.g., Dobkowski's correlation function,[26] suggesting a close relation between thermodynamic properties and dynamics. One system property of technological significance for estimating the mechanical and dynamical properties of a material is glass transition temperature, T_g.[27–30] With regard to polymers, it has been known for some time that in addition to the chemical structure of the monomer, T_g scales inversely with the number average molecular weight for low molecular weight polymers. Several chain-length dependence correlation functions for estimating T_g have been proposed for linear polymer chains.[31–34] The central idea behind these correlations is that linear polymer chains of different lengths exhibit the same free volume at T_g while the chains ends contribute excess free volume. It should be noted that the molecular intra-molecular heterogeneous behavior is based on the intra-molecular characteristics and thus different from the heterogeneity near the glass transition temperature, T_g, where in spacial domains, the dynamics vary spatially and temporally.[28,35,36] Although for linear chains, there is a satisfactory understanding of the underlying mechanism in the proximity of T_g, for star-shaped macromolecules is complicated and poorly understood.[37] Roovers and Toporowski have shown that T_g follows quantitatively the end-group concentration dependence without taking into account the branching point.[38] However, Rietsch and co-workers have presented results that show that the branching at the core particle is more important than the chain ends.[39] The difference between the data in the literature has been suggested to be due to the chemical structure at the core particle.[40] There are important unresolved questions associated with the property dependence on the functionality and the molecular weight per arm of star-shaped polymers in the fluid phase near T_g.

The aim of the current paper is the study of the density, the packing properties, and the structural relaxation times for different parts of the molecular structure of star polymer melts in the fluid state. Moreover, we estimate the isokinetic temperature at the time-scale of the laboratory glass-transition by extrapolating from the characteristic molecular relaxation time associated to the spontaneous fluctuations at equilibrium at different temperatures; this dynamic description of T_g does not represent a loss of thermodynamic equilibrium. Thus, up to the computational feasible point where the decay of the system's structural relaxation can be observed, we capture how the molecular architecture of polymeric fluids affects the structural and dynamical properties as temperature is decreased towards T_g. We use molecular dynamics simulations (MD) with a bead-spring model, which takes into account the space-filling effects. We focus on molecular architectures that have a minimum influence from the size of the core particle; the size of the core particle can have significant structural (and subsequently dynamical) effects[41] and they are subject of future work. To organize our findings, we generalize Dobkowski's correlation function[26] to include star polymers by using the arm length, M, rather than the chain length as the main parameter in the correlation:

$$Q(M) = Q_\infty - \frac{K}{M + M^*}, \tag{1}$$

where Q is a structural or dynamical property and Q_∞ is the value of Q at infinite arm length. K and M^* are empirical constants. Overall, the obtained results show a non-trivial link between the structure and dynamics of star polymers, where both the functionality and the arm length can significantly affect the system properties under investigation.

The paper is organized as follows. Section II contains details of the model and the simulation methods. Results for the structure and dynamics of star polymers are presented in Sec. III. Section IV concludes the report.

II. MODEL AND METHODOLOGY

The system consists of $N_s = 400$ polymers. A star polymer is represented as a spherical core with f attached arms and each arm is composed of M beads. The architecture parameters that we have investigated are for arm lengths $M = 5$, 10, 20, and 40 and for functionalities $f = 2$, 4, 6, 8, 12, and 16. Interactions between polymer beads are described by the cut-and-shifted Lennard-Jones (LJ) potential with ε and σ as the energy and range parameters, and the cutoff distance $r_c = 2.5\sigma$. The beads along a chain are connected with their neighbors via a stiff harmonic spring, $V_H(r) = k(r - l_0)^2$, where $l_0 = 0.99\sigma$ is the equilibrium length of the spring and $k = 5000\varepsilon/\sigma^2$ is the spring constant. The core–core and core–monomer interactions are modeled as purely repulsive Weeks-Chandler-Andersen potential[42] with modification taking into account the difference in the particle sizes.[43] We set the diameter of the polymer beads as the unit of length, σ; the core radius is $R_c = 0.25\sigma$. The mass of a particle scales linearly with volume, so that m_b and $m_c = 0.125m_b$ for the mass of the polymer bead and core, respectively. We focus on small core particle size to ensure that no anisotropic aggregation occurs in our systems.[41] The energy and interaction range parameters are chosen to be the same for these interactions such that $\varepsilon_{cc} = \varepsilon_{cb} = \varepsilon$ and $\sigma_{cc} = \sigma_{cb} = \sigma$. For a linear chain, which is denoted as a star polymer with $f = 2$, the core is of the same type as the beads composing the arms. Typical molecular configurations are shown in Fig. 1.

Simulations were performed in a cubic box with length L; periodic boundary conditions and the minimum-image convention were applied in all three directions. The simulations were performed by the large-scale atomic/molecular massively parallel simulator (LAMMPS) developed at Sandia National Laboratories.[44] Simulations were performed in the *NVT* ensemble after equilibration in the *NPT* ensemble at the desired temperature. The equilibration at the *NPT* ensemble

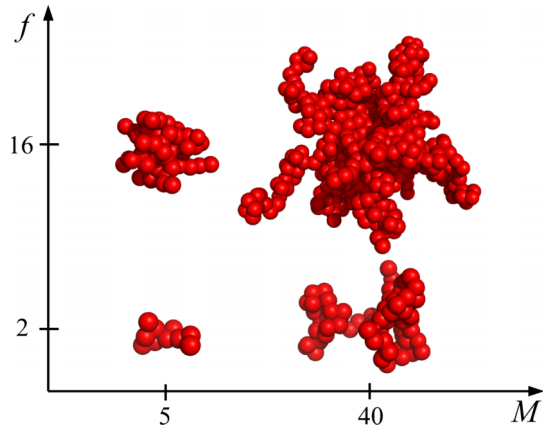

FIG. 1. Schematic displaying typical molecular configurations of star polymers at different molecular architectures.

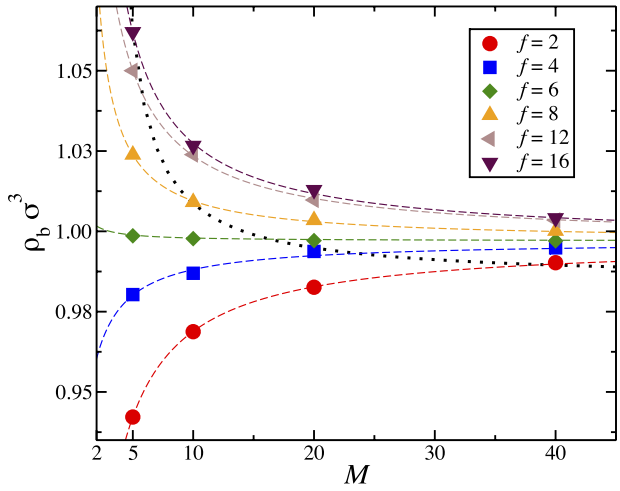

FIG. 2. Number bead density, ρ_b, of star polymer melts at $T = 0.5$ and $P = 0$ as function of arm length, M, for functionality, f. The dashed lines correspond to fits to Eq. (1) for different functionalities. The dotted line corresponds to a fit to stars with $fM = 80$, i.e., the points $(f, M) = (2, 40)$, (4, 20), (8, 10), and (16, 5). The parameters of the fits for different values of f are shown in Table I.

was necessary to avoid negative pressure with temperature variation.[45] Time averaging was conducted for $O(10^8)$ time steps after equilibration. The time step was set to $\delta t = 0.005\tau$, where $\tau = \sigma(m_b/\varepsilon)^{1/2}$ is the unit of time. Temperature and pressure are measured in units of ε/k_B and σ^3/ε, respectively. k_B is Boltzmann's constant. All simulations were performed at $P = 0$ in reduced units, which closely corresponds to atmospheric pressure.

III. RESULTS & DISCUSSION

When a star polymer is compared to a linear polymer of the same molecular weight, two opposing effects can be identified: an increased number of arms will increase the free volume and thus enhancing the mobility, but on the other hand, mobility would be restricted by the branched core particle. Thus, to understand the behavior of relaxation behavior as the molecular architecture changes to start the investigation on the physical properties of star polymers. In particular, we focus on the number bead density in the interstitial space between the cores, $\rho_b = N_s f M/(L^3 - N_s \frac{4\pi}{3} R_c^3)$. The results for ρ_b offer insights for the number density of free ends, ρ_{free}, since $\rho_b = M\rho_{free}$. Results for ρ_b at $T = 0.5$ are shown in Fig. 2. The parameters obtained from the fitting with Eq. (1) are shown in Table I. A single value of $\rho_{b,\infty}$ has been found to describe the behavior for all functionalities, suggesting that there is no difference in density between linear and star polymers at infinite long arms. Linear chains ($f = 2$) and star polymers with $f = 4$ display an increase of ρ_b with increasing arm length, which is consistent with the idea that increasing the arm length would lead to denser systems. However, for star polymers with $f \geq 6$, as the arm length increases ρ_b decreases; for $f = 6$, the effect was small. Nevertheless, the overall behavior can still be described by Eq. (1), see Fig. 2. An increase of f for star polymers of the same molecular weight, e.g., $fM = 80$, leads to an increase in ρ_b. For star polymers of the same molecular weight, this signifies that an increase in f leads to a decrease of the volume per free end $\sim \rho_{free}^{-1}$. In other words, an increase in the number of free ends leads to the volume per particle increases; this is the opposite effect from what is understood for linear chain melts. Nevertheless, this is consistent with the physical picture that branching leads to molecular contraction, which in turn decreases the critical temperature and increases the critical polymer volume fraction.[46] The specific volume, $v = 1/\rho_b$, for all molecular architectures had a linear dependence on temperature; results of linear fits are presented in Table II. However, higher functionalities and longer arms led to smaller dependence on temperature. This is also consistent with the physical picture that a molecule larger in size (in our case, either by increasing f and/or M) becomes less sensitive to temperature variation.

The ρ_b behavior of stars (for short arms) appears to challenge the assumption that chain ends contribute excess free volume, but a closer look on the architecture is required. In the Daoud-Cotton model,[10] the concentration at the core is the highest than in other regions and it is fixed throughout the core region. The blob size coincides with the monomer size and the arms are completely stretched. The size of the core region of a star depends on the functionality ($d_{core} \sim f^{1/2}$), but not on the arm length. More arms would result in a larger core region, but as the arm length gets shorter, the core region becomes more prominent. Since the core region is described with a density higher than the other regions, the decrease of arm length would result in systems with higher density. The manifestation of a dominant core region also affects the way arms (belonging to the same star) would distribute themselves from the core particle, $\rho_{arm}(r)$; higher f leads to a more structured distribution with a slower decay with distance from the core particle, see inset in Fig. 3. Although the effect appears to be small in the density distribution of the brushes, f has a significant impact on the organization of the stars in the melt. The first important observation is that linear chains have more ordered structure based on the behavior of radial distribution function between core particles, $g_{cc}(r)$ than $f = 4$ star polymers, see Fig. 3. This does not contradict previous conclusion that linear chains can be described as a fluid of soft particles.[47] The main difference is that we calculate the radial distribution of only the core particle rather than the molecular center of mass,

TABLE I. Parameters obtained from fitting Eq. (1) to ρ_b (see Fig. 2), the isokinetic temperature for the star's core particles, T^c_{iso}, and the isokinetic temperature of the star's free ends, T^e_{iso} at the structural relaxation time of 100 s.

	$Q(M) = \rho_b, T = 0.5$			$Q(M) = T^c_{iso}$			$Q(M) = T^e_{iso}$		
f	$\rho_{b,\infty}$	K	M^*	$T^c_{iso,\infty}$	K	M^*	$T^c_{iso,\infty}$	K	M^*
2	0.997	0.289	0.27	0.381	1.155	37.27	0.381	1.227	39.01
4	0.997	0.094	0.58	0.374	0.135	9.42	0.377	0.334	24.38
6	0.997	−0.009	−0.03	0.368	−0.208	−0.07	0.372	−0.097	−2.37
8	0.997	−0.117	−0.65	0.372	−0.286	0.48	0.368	−0.343	1.86
12	0.997	−0.265	−0.02	0.336	−0.652	1.46	0.331	−0.616	0.92
16	0.997	−0.286	−0.60	0.295	−1.364	5.30	0.293	−1.452	6.21

which offers an average description of the whole molecule. For linear chains, the core particles can be in close proximity, since there is considerable overlap between the chains. The difference between $f = 2$ and $f = 4$ displays the impact caused by the branching, which leads the core particles for stars $f = 4$ to larger distances reducing the degree of order initially observed for linear chains. As functionality increases ($f > 4$), the distance between core particles increases further, but now, the degree of order increases. That is because the stars become less soft and there is less penetration/overlap by neighboring stars. The increase in the degree of order between the core particles for the functionalities explored did not form crystal structures. The difference between low functionalities ($f = 2$ and 4) and higher functionalities ($f > 6$) signals the crossover from polymer-like to star-like behavior.

One may get more information on the structure and packing of star polymers in melt conditions by counting a star polymer's neighbors in contact. To identify a pair of beads in contact, we used a distance criterion between the beads, $d = 1.4\sigma$. We only consider beads belonging to different star polymers. Based on this criterion, the following two quantities are measured. The first quantity is the number of molecular neighbors in contact, n_{mol}, and the second one is the number of polymer beads in contact, n_b. The calculated values for n_b and n_{mol} are presented in Table II. The ratio of n_b over n_{mol} would correspond to the average number of hetero-contacts per molecular neighbor. The ratio for all the molecular architectures collapses on a master curve when plotted as function of the scaled product of $f^{0.84}M^{0.68}$, Fig. 4. The exponents are determined via an empirical fit to the simulation results.

TABLE II. The temperature dependence of the specific volume is fitted to a linear relation, $v = 1/\rho_b = \alpha T + \beta$ as well as the average number of molecular (n_{mol}) and bead (n_b) neighbors is presented. Additionally, the relevant VFT parameters obtained from fitting to Eq. (3) are also presented for the core particle and free ends.

						Core particle			Free ends		
M	f	α	β	n_{mol}	n_b	τ^c_v	E^c	T^c_v	τ^e_v	E^e	T^e_v
5	2	0.345	0.888	9.04	38.44	0.6	0.88	0.327	0.6	0.88	0.327
5	4	0.317	0.862	9.78	72.08	2.1	0.84	0.338	1.1	0.81	0.341
5	6	0.297	0.853	9.77	101.07	16.0	0.88	0.380	4.0	0.88	0.380
5	8	0.271	0.840	9.55	122.72	22.1	1.02	0.389	4.9	1.04	0.384
5	12	0.256	0.821	9.02	161.88	56.0	1.08	0.399	10.1	1.08	0.399
5	16	0.275	0.800	8.55	192.44	123.0	1.10	0.387	17.2	1.10	0.385
10	2	0.325	0.869	11.09	73.69	1.6	0.91	0.327	1.6	0.91	0.327
10	4	0.305	0.858	12.15	137.71	6.0	0.91	0.337	2.3	0.87	0.338
10	6	0.292	0.856	12.15	192.05	35.0	0.91	0.358	10.5	0.84	0.358
10	8	0.289	0.844	11.96	239.73	72.7	0.94	0.366	12.4	0.90	0.368
10	12	0.279	0.836	10.98	318.17	174.0	1.02	0.356	22.6	1.01	0.354
10	16	0.274	0.834	10.34	388.62	354.0	1.05	0.345	31.9	1.05	0.345
20	2	0.291	0.872	13.27	146.49	3.0	0.97	0.330	3.0	0.97	0.330
20	4	0.305	0.853	15.32	266.79	24.0	0.88	0.340	8.9	0.85	0.342
20	6	0.294	0.855	15.51	375.46	55.0	0.89	0.345	10.5	0.89	0.343
20	8	0.286	0.853	15.01	471.99	230.0	0.89	0.352	27.6	0.89	0.351
20	12	0.287	0.845	14.06	641.44	500.0	1.20	0.320	47.5	1.10	0.320
20	16	0.285	0.844	13.15	790.66	770.0	1.30	0.297	4.6	1.20	0.310
40	2	0.301	0.860	17.16	269.39	12.0	0.97	0.333	12.0	0.97	0.333
40	4	0.302	0.854	18.36	505.81	84.5	0.84	0.341	84.5	0.84	0.341
40	6	0.292	0.857	17.00	699.36	315.0	0.77	0.345	50.4	0.77	0.350
40	8	0.291	0.854	16.89	887.79	780.8	0.82	0.348	78.1	0.82	0.348
40	12	0.293	0.849	16.91	1260.39	2000.0	1.12	0.307	88.0	1.12	0.307
40	16	0.285	0.852	15.53	1562.15	2400.0	1.50	0.264	72.0	1.50	0.270

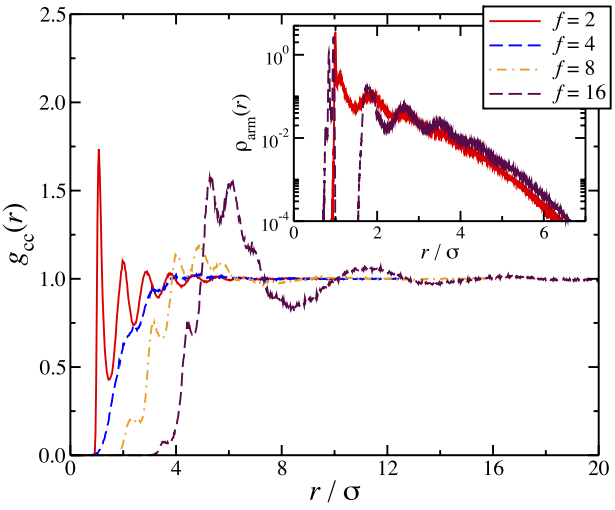

FIG. 3. Radial distribution function between core particles for star polymer melts with $M = 10$ at $T = 0.65$. The inset displays the average number bead density distribution of the arms of a single star polymer in melt conditions as function of distance from its core particle.

The collapse of the data to this empirical fit may reflect the fractal nature of star polymer melts. One observation is that the number of bead hetero-contacts per molecular neighbor increases with increasing M and f, though the ratio n_b/n_{mol} increases at a higher rate with f rather than with M. A possible explanation is due to the packing between the star polymers. Both n_b and n_{mol} (as seen in Table II) increase with increasing M, which results in a moderate increase in n_b/n_{mol}. On the other hand, increasing f results in an increase in n_b as expected, but at the same time, there is a decrease in n_{mol}. The physical picture for this is that higher values of f correspond to more compact molecular conformations and thus, it is less likely for a star to be able to be in contact with a large number of neighbors.

Having established the effect of f and M of star polymers on their structural/morphological properties, we now turn our attention to the dynamics of these systems. We do so by calculating the structural relaxation (or α-relaxation) time, τ_α

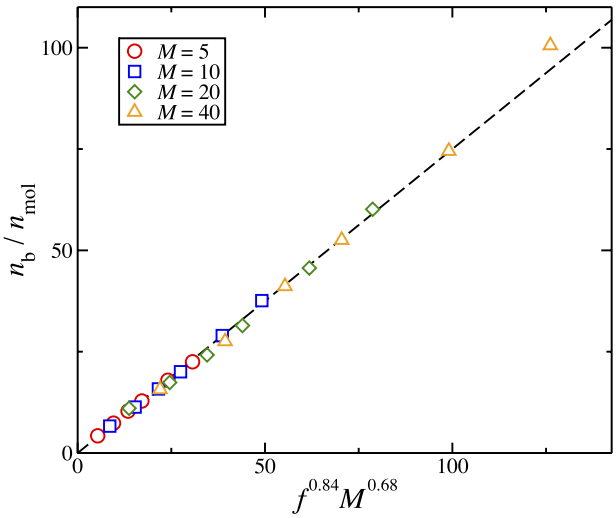

FIG. 4. Average number of bead hetero-contacts over the average number of molecular neighbors, n_b/n_{mol}, as function of the product $M^{0.68}f^{0.84}$ at $T = 0.5$. The dashed line is a guide for the eye.

of the macromolecules above T_g. The τ_α is evaluated by the intermediate scattering function F, which is an experimentally observable quantity that measures the decay of density fluctuations.[48] The function is written as

$$F(q,t) = \frac{1}{N}\sum_{j=0}^{N}\langle \exp\{i\mathbf{q}\cdot[\mathbf{r}^j(t+t') - \mathbf{r}^j(t')]\}\rangle. \quad (2)$$

The wave number q in $F(q,t)$ can take on a range of values to reflect the decay of different Fourier modes of the particle density correlations. However, following a common choice, we consider the wavenumber corresponding to the first maximum in the static structure factor $S(q)$.[49] Intuitively, the particular choice reflects the relevant length scale characterizing a "cage effect" in the liquid. For $f = 2$ and 4, the first peak is located at $q\sigma \approx 7$ reflecting a segmental description and no identifiable peak at the molecular level was found, which is consistent with previous studies.[45] However, for star polymers ($f > 4$), the first peak appears at q-values associated with the size of the star polymer, $q\sigma \approx 1$. Hence, for consistency, we have used the radius of gyration, R_g, of the macromolecule to define the wavelength, $q = 2\pi/R_g$, for the cases $f = 2$ and 4. This reflects a molecular rather than a segmental characteristic length scale, which is similar to the size of the molecule. Irrespective of the choice, the results would not qualitatively be affected. Moreover, to provide a simpler measure of the decay of density correlation, we define a structural relaxation time, τ_α, as the time at which the correlations have decreased by a factor of e, i.e., $F(q,\tau_\alpha) = 1/e$.

The key question is how the star-shaped architecture affects the distribution of segment dynamics at the vicinity of the core particle or at the free end of the arm. Adams *et al.* showed that there is a distribution of time scales along an arm of a star polymer and demonstrated this with a four-arm star melt by selectively labeling different parts along an arm and studied their dynamics.[7] In particular, their findings show that the monomers near the free ends have faster relaxation times than the monomers near the star's core. This effect has been observed in oligomer-grafted nanoparticles,[50,51] where there was a significant slow down in the segmental dynamics for the segments near the core particle and as a result affecting the macroscopic properties of the material. In our investigation, the dynamical behavior of the segments at different locations along an arm (grafted chain) is presented in Figs. 5(a) and 5(b). The structural relaxation time of selected beads along the arm significantly depends on the location of the particular bead from the core particle, y. For the star-melts with $M = 40$, it becomes clear that there are three regimes, each corresponding to the core, middle, and free-ends regions. For $M = 40$, these regimes are located as follows: in close proximity to the core particle ($y < 5$) as well as near the free-ends ($y > 37$), there is a decrease τ_α, while the middle regime corresponds to an observed plateau for τ_α ($5 < y < 37$). Higher values of f enhance the differences between the three regimes, Fig. 5(a). The small differences observed between the free ends and the middle of linear chains ($f = 2$) are consistent with findings of a previous study.[8] The middle regime shrinks in size as the arm length decreases and for short arm lengths ($M = 5$ and 10), no plateau is observed, Fig. 5(b). The difference in the

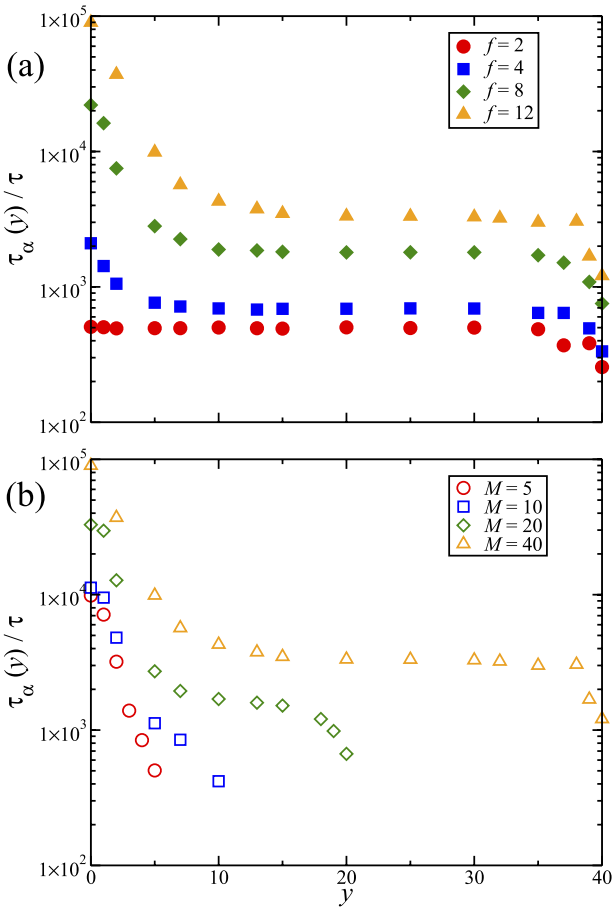

FIG. 5. Structural relaxation time, τ_α, along a grafted chain at $T = 0.5$ for (a), $M = 40$ at different values of f and for (b), $f = 12$ at different values of M. The values of y correspond to the position of the bead y along the arm with $y = 0$ and $y = M$ being the core particle and the free-end, respectively.

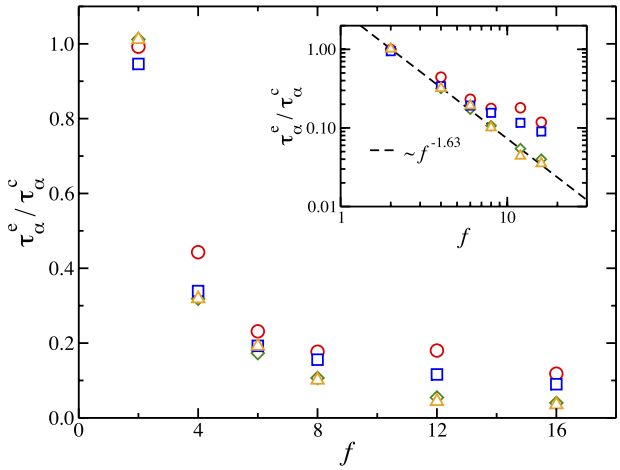

FIG. 6. Structural relaxation time ratio, $\tau_\alpha^e/\tau_\alpha^c$, as function of functionality, f, at $T = 0.5$; symbols correspond to stars with $M = 5$ (circles), $M = 10$ (squares), $M = 20$ (diamonds), and $M = 40$ (triangles). The dashed line corresponds to $\sim f^{-1.63}$.

dynamics between the core particles, τ_α^c, and the dynamics of the free-ends, τ_α^e, highlights a star's dynamical behavior at these opposing boundaries; it would be discussed below with focus on the iso-kinetic temperature. The magnitude of the difference between the two types of relaxation can be described by the ratio of $\tau_\alpha^e/\tau_\alpha^c$. As functionality increases, the two types of relaxation times become significantly different, Fig. 6. The ratio, $\tau_\alpha^e/\tau_\alpha^c$, follows a power-law dependence with functionality, i.e., $f^{-1.63}$, see inset in Fig. 6. Deviation from this dependence is observed for high values of f and short arms. At the deviation, the molecular characteristics of the star resemble more of a shape-able sphere with a small degree of inter-penetration rather than a highly penetrable soft sphere, for typical molecular configuration of $f = 16$, see Fig. 1. Overall, the findings suggest that functionality enhances the intra-molecular heterogeneity in time scales of a polymer melt.

We continue with examining further the dynamical behavior of the core particle, since it has the slowest relaxation time in the molecular structure. This means that the overall behavior of the system at length scales larger than the molecular structure would be closely associated with the core particle rather than the free-ends. For high temperatures, an increase of f results in several orders of magnitude higher values of τ_α^c, see Fig. 7(a). This is understandable since the size of the star becomes larger with f. For lower temperatures, τ_α^c increases significantly, but for high values of f, this increase is more gradual suggesting smaller sensitivity to temperature variation. This is also in agreement with the density dependence on temperature at different functionalities, see Table II. A complementary perspective is the molecular architecture dependence at a fixed temperature. Results for $T = 0.5$ at different molecular parameters are presented in Fig. 7(b). From comparisons with the density at the same conditions, Fig. 2, it is clear that τ_α^c follows similar trends with density. For $f = 2$ and 4, τ_α^c increases monotonically with M, which is consistent with the idea that longer arms reduce the system's free volume and thus the dynamics of the molecules. On the other hand, there is a minimum at τ_α^c as function of M for $f \geq 6$, Fig. 7(b). A possible interpretation for the minimum comes from the balance of two factors. The first factor is the density. For $f \geq 6$ and small M, the density is significantly high (Fig. 2), which means that there is less free volume in the system causing considerable hindrance to the mobility of the stars. The second factor is the impact of arm length on the dynamics. As M increases, the density drops allowing the polymer beads to relax faster, explaining the initial drop of τ_α^c. However, the relaxation of the core particle depends also on the relaxation of the arms and a longer arm requires longer time to relax, and thus, τ_α^c increases for long arms. The minimum is the balance between these two factors.

The structural relaxation time for fluids is usually fit by the well-known Vogel-Fulcher-Tammann (VFT) relation[52–54]

$$\tau_\alpha = \tau_v \exp\left(\frac{E}{T - T_v}\right), \tag{3}$$

where E and T_v are parameters with dimensions of temperature and τ_v is the characteristic relaxation time for high values of temperature. T_v is an extrapolated divergence T of τ also known as the Vogel temperature and is typically 30–50 K below the glass-transition temperature. The resulting parameters are presented in Table II. The values of E and T_v for the free-ends and the core particles have similar values suggesting (aside the statistical errors) that at temperatures near

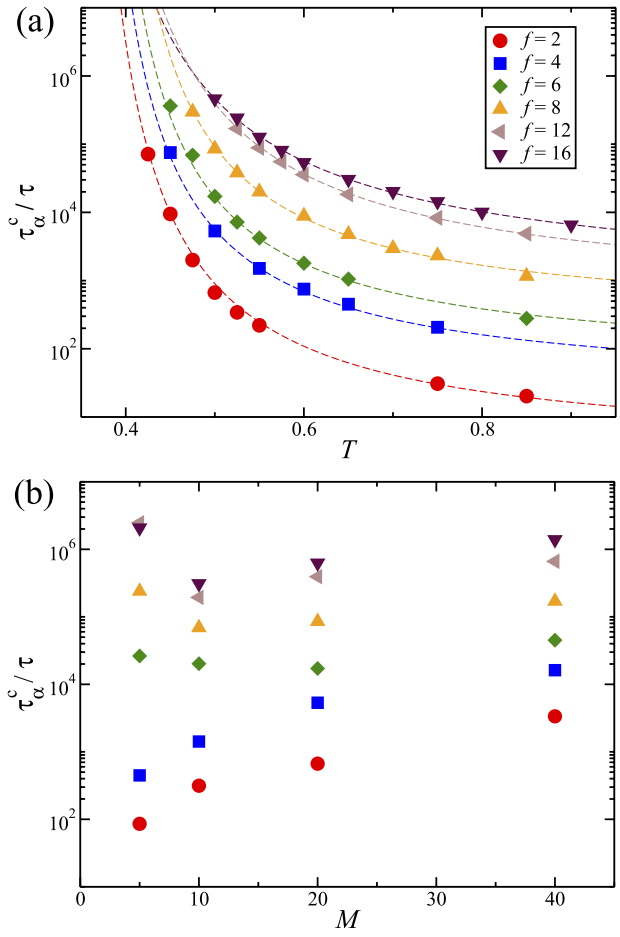

FIG. 7. (a) Core particle's structural relaxation time, τ_α^c, as function of temperature, T, for stars with $M = 20$. Results for different functionalities are also presented. The dashed lines correspond to fits to Eq. (3). (b) Core particle's structural relaxation time, τ_α^c, as function of the arm length, M, at $T = 0.5$. The symbols are the same as in (a).

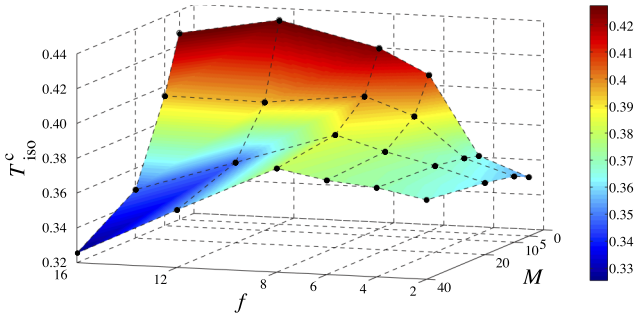

FIG. 8. Isokinetic-temperature for star's core particle, $T_{iso}^c(\tau_\alpha^c = 100$ s), as function of arm length, M, and functionality, f.

T_v, they have relaxation times at the same level. Indeed, the main difference between the two types of relaxation times is for τ_v, which is the characteristic relaxation time at high temperatures. The key significance from these observations is that the molecular architecture significantly affects the dynamics of a polymer system and thus becoming an option in the design of soft materials with the desired properties. To estimate T_g, a common practice is for the data to be fitted to Eq. (3). T_g is equated to the isokinetic temperature based on the condition that $\tau_\alpha = 100$ s (the canonical definition of the laboratory glass-transition[55]) assuming that one time unit in standard LJ reduced units corresponds to $\tau = 10^{-12}$ s. For the purposes of the current investigation, we focus the relaxation time of the core particle, since being the slowest relaxation time, it becomes a good indicator on when the whole molecule can be considered relaxed. In other words, we assume that the glass transition temperature is in the vicinity of $T_{iso}^c(\tau_\alpha^c = 100$ s).

We calculate the isokinetic temperature for the core particle, $T_{iso}^c(\tau_\alpha^c = 100$ s), and we find that it is significantly affected by both f and M in a non-trivial fashion, see Fig. 8. The overall behavior is similar to that of ρ_b, compare Figs. 2 and 8. This reflects a subtle and close relation between the structural and dynamical properties; both ρ_b and T_{iso}^c depend on the arm length variation as $\sim M^{-1}$. Nevertheless, the parameters in the correlations, i.e., K, M^*, have a non-trivial dependence on f signifying that the role of the branched core particle is also significant, e.g., the parameter K determines the slope of $Q(M)$. For $f < 6$, an increase of M leads to an increase for both ρ_b and T_{iso}^c, see Figs. 2 and 8, respectively; this regime is associated with linear melt type of behavior. For $f > 6$, there is a crossover, now both T_{iso}^c and ρ_b decrease with M. Here, two regimes can be identified. The first one is the small corona regime, which is observed for high functionality and short arms ($f > 6$ and $M \leq 10$). The molecular structure is dominated by the core region resulting to a highly compact configuration with little overlap by its neighbors. In other words, a star polymer resembles a colloidal-like particle and in the proximity to T_g, the mobility of a star would be better described by the caging mechanism, which is well known in colloidal science and it is responsible for glass transition and/or jamming.[56] In this regime, the $\tau_\alpha(y)$ does not have the plateau observed in longer arms as discussed above, see also Fig. 5(b). Moreover, the highest values of ρ_b and T_{iso} are observed in this regime. The second regime includes the rest of the parameter space ($f > 6$ and $M > 10$). Increasing arm length has as a consequence: the formation of a soft corona around the core region, and leading to a significant reduction of ρ_b (as discussed above, also see Fig. 1) and T_{iso}^c with respect to the previous regime. The formation of a soft corona around the core region is evident in the dynamical behavior of the segments along the arms. Indeed, as discussed above, for $f > 6$ and $M > 10$, a plateau is observed in the segmental relaxation times along the arms clearly separating the three regimes (namely, the core regime, the middle, and the free ends), as seen in Figs. 5(a) and 5(b). This highlights a close relation between the segmental relaxation of the arms and the core particle. For long arms, $M = 20$ and 40, ρ_b is at the same level with a small variation, where higher functionality still leads to higher density. One the other hand, T_{iso}^c for high functionalities and long arms is significantly lower than their linear counterparts. This is consistent with findings of previous experimental studies.[37,57] At this point, it is important to note that this effect is not due to the increased free volume caused by an increased number of free-ends into the system. If that would be true, then decreasing the length of the arms would further decrease T_{iso}^c, which is not consistent to our findings as presented above. Instead, a possible interpretation for systems that belong to this particular regime (long arms and high functionality) is that even though these systems have lower

free volume (higher density), its distribution is concentrated at the free-ends permitting a star polymer to flow between its neighbors with less difficulty than linear melts at the same conditions. This coincides with a low value of the ratio $\tau_\alpha^e/\tau_\alpha^c$ meaning that the free ends have significantly lower relaxation times than the core particle, see Figs. 5 and 6. In other words, a softer corona effectively filters the caging effects from the core (high-density) regions of neighboring stars, permitting a star polymer to escape from the cage at shorter time scales; an equivalent effect observed in simulations of grafted nanoparticles in the absence of solvent.[58] Our results appear to be in agreement with the experimental findings by Rietsch *et al.* (see Fig. 2 in Ref. 39). Nevertheless, our findings suggest that both the free-ends and the branching core particle are significant. The free-ends play a dominant role at low values of f, while for $f \geq 6$, the branching takes over. The obtained results may be used as a reference of the ideal physical behavior of a star melt and any deviation observed would be due to the local/specific chemistry.

To finish our discussion, we focus on the significance of the unit of time. In the above calculations, we have used $\tau = 10^{-12}$ s, which has been used in the past.[59] It is essentially a characteristic time scale associated with the atomistic characteristics of the monomers and a map between our model and an experimental system. Depending on the map, different characteristic time units may be used, which may have an order of magnitude difference depending on the stiffness of the polymeric chain.[3] However, our choice here is arbitrary and a different value may have a qualitative impact in the calculation of the isokinetic temperature, as presented above. To illustrate this subtle point, we choose star polymers with $M = 40$ and compare the $T_{iso}^c(\tau_\alpha^c = 100\ \text{s})$ for two different time units, namely, $\tau = 10^{-12}$ s and $\tau = 10^{-6}$ s, see Fig. 9. In both cases, as f increases, T_{iso}^c increases up to $f = 8$, where the behavior is reversed. A higher value of the time unit results in larger isokinetic temperature values as one would expect. The shift of higher isokinetic temperatures for $f \leq 8$ is without significant qualitative deviations in the rate of change with f. Nevertheless, for $f > 8$, the decrease of T_{iso}^c becomes less sharp as the unit of time increases. For a higher value, for the unit of time, high functionality stars have equivalent T_{iso}^c values with their linear polymer counterparts, while for a lower value of τ, stars of high functionality lead to systems with higher mobility with respect to linear polymer melts. This highlights that the local (chemical) structure is important and care is needed when star polymers of different chemical composition are compared.

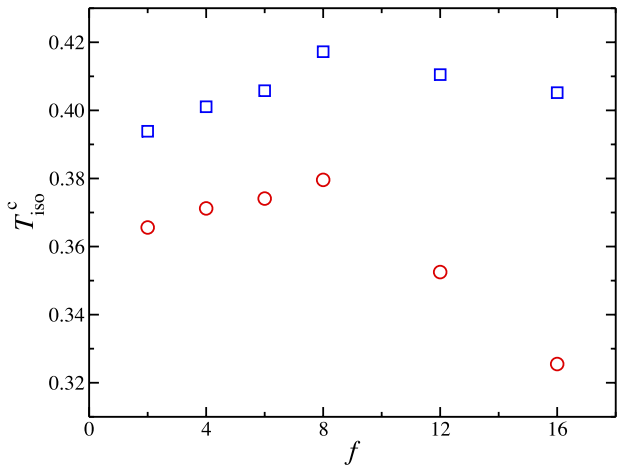

FIG. 9. Isokinetic-temperature for star's core particle, $T_{iso}^c(\tau_\alpha^c = 100\ \text{s})$, with $M = 40$ as function of functionality, f. The symbols correspond to different values of the unit of time: circles for $\tau = 10^{-12}$ s and squares for $\tau = 10^{-6}$ s.

IV. CONCLUSIONS

In summary, molecular dynamics simulations of a bead-spring model were used in a systematic way to gain insights into the structural and dynamical behavior of star-shaped polymer melts at fixed pressure. In particular, a number of quantities were calculated, namely, the density, packing properties, as well as the structural relaxation times for the core and free-end particles. We rationalized our findings in terms of the hierarchy of motions inherited by the asymmetry in the star molecular architecture. Moreover, the isokinetic temperature is estimated at the time-scale of the laboratory glass-transition based on the measured structural relaxation times. To organize the results for the density and isokinetic temperature, we have modified Dobkowski's chain-length dependence correlation function for star polymers. For linear chain polymers and low functionality stars, an increase of arm length would result in an increase of the densities and the glass-transition temperatures, which is consistent with previous studies. High functionality stars exhibited the opposite behavior, that is, an increase of the arm length would lead to a decrease of the densities and the glass-transition temperatures. The difference in the properties between low and high functionality stars is more pronounced for short arm lengths. Our findings would be valuable in the design and manufacture of polymeric and nanocomposite materials with the desired properties.

ACKNOWLEDGMENTS

The authors would like to thank to Dr. P. J. Camp, Professor C. N. Likos, and Professor A. Z. Panagiotopoulos for insightful discussions. A.C. is thankful for computational resources provided by Panagiotopoulos Group and Imperial College London. E.G. and P.F.G. are thankful for support from National Science Foundation (NSF), Division of Materials Research (No. DMR-1305749).

[1]P. G. de Gennes, *Scaling Concepts in Polymer Physics* (Cornell University Press, Ithaca, 1979).
[2]P. G. de Gennes, J. Chem. Phys. **55**, 572 (1971).
[3]K. Kremer and G. S. Grest, J. Chem. Phys. **92**, 5057 (1990).
[4]L. Fetters, A. D. Kiss, D. S. Pearson, G. F. Quack, and F. J. Vitus, Macromolecules **26**, 647 (1993).
[5]S. T. Milner and T. C. B. McLeish, Phys. Rev. Lett. **81**, 725 (1998).
[6]S. T. Milner and T. C. B. McLeish, Macromolecules **30**, 2159 (1997).
[7]C. H. Adams, M. G. Brereton, L. R. Hutchings, P. G. Klein, T. C. B. McLeish, R. W. Richards, and M. E. Ries, Macromolecules **33**, 7101 (2000).
[8]A. Bormuth, P. Henritzi, and M. Vogel, Macromolecules **43**, 8985 (2010).
[9]T. Pakula, Comput. Theor. Polym. Sci. **8**, 21 (1998).
[10]M. Daoud and J. P. Cotton, J. Phys. **43**, 531 (1982).
[11]G. S. Grest, L. J. Fetters, J. S. Huang, and D. Richter, Adv. Chem. Phys. **94**, 67 (1996).
[12]T. C. McLeish, Adv. Phys. **51**, 1379 (2002).
[13]C. N. Likos, Soft Matter **2**, 478 (2006).
[14]D. Vlassopoulos and G. Fytas, Adv. Polym. Sci. **236**, 1 (2010).

[15]K. Binder and A. Milchev, J. Polym. Sci., Part B: Polym. Phys. **50**, 1515 (2012).
[16]C. N. Likos, H. Löwen, M. Watzlawek, B. Abbas, O. Jucknischke, J. Allgaier, and D. Richter, Phys. Rev. Lett. **80**, 4450 (1998).
[17]M. Watzlawek, C. N. Likos, and H. Löwen, Phys. Rev. Lett. **82**, 5289 (1999).
[18]G. S. Grest, Macromolecules **27**, 3493 (1994).
[19]R. Seghrouchni, G. Petekidis, D. Vlassopoulos, G. Fytas, A. N. Semenov, J. Roovers, and G. Fleischer, Europhys. Lett. **42**, 271 (1999).
[20]D. Vlassopoulos, G. Fytas, S. Pispas, and N. Hadjichristidis, Physica B **296**, 184 (2001).
[21]E. Glynos, A. Chremos, G. Petekidis, E. Theofanidou, P. J. Camp, and V. Koutsos, Macromolecules **40**, 6947 (2007).
[22]F. L. Verso, S. A. Egorov, A. Milchev, and K. Binder, J. Chem. Phys. **133**, 184901 (2010).
[23]A. Chremos, E. Glynos, V. Koutsos, and P. J. Camp, Soft Matter **6**, 1483 (2010).
[24]H.-Y. Yu and D. L. Koch, Langmuir **26**, 16801 (2010).
[25]M. Rubinstein and R. H. Colby, *Polymer Physics* (Oxford University Press, Oxford, 2003).
[26]Z. Dobkowski, Eur. Polym. J. **18**, 563 (1982).
[27]C. A. Angell, K. L. Ngai, G. B. McKenna, P. F. McMillan, and S. W. Martin, J. Appl. Phys. **88**, 3113 (2000).
[28]H. Sillescu, J. Non-Cryst. Solids **243**, 81 (1999).
[29]P. G. Debenedetti and F. H. Stillinger, Nature **410**, 259 (2001).
[30]F. H. Stillinger and P. G. Debenedetti, Annu. Rev. Condens. Matter Phys. **4**, 263 (2013).
[31]T. G. Fox and P. J. Flory, J. Appl. Phys. **21**, 581 (1950).
[32]T. G. Fox and P. J. Flory, J. Polym. Sci. **14**, 351 (1954).
[33]R. W. Douglas and B. Ellis, *Amorphous Materials* (Wiley-Interscience, New York, 1972).
[34]Y. W. Kim, J. T. Park, J. H. Koh, B. R. Min, and J. H. Kim, Polym. Adv. Technol. **19**, 944–946 (2008).
[35]J. F. Douglas and J. B. Hubbard, Macromolecules **24**, 3163 (1991).
[36]C. Donati, J. F. Douglas, W. Kob, S. J. Plimpton, P. H. Poole, and S. C. Glotzer, Phys. Rev. Lett. **80**, 2338 (1998).
[37]Z. Qian, V. S. Minnikanti, B. B. Sauer, G. T. Dee, and L. A. Archer, Macromolecules **41**, 5007 (2008).
[38]J. E. L. Roovers and P. M. Toporowski, J. Appl. Polym. Sci. **18**, 1685 (1974).
[39]F. Rietsch, D. Daveloose, and D. Froelich, Polymer **17**, 859 (1976).
[40]A. Hale, C. W. Macosko, and H. E. Blair, Macromolecules **24**, 2610 (1991).
[41]A. Chremos and A. Z. Panagiotopoulos, Phys. Rev. Lett. **107**, 105503 (2011).
[42]J. D. Weeks, D. Chandler, and H. C. Andersen, J. Chem. Phys. **54**, 5237 (1971).
[43]J. S. Smith, D. Bedrov, and G. D. Smith, Compos. Sci. Technol. **63**, 1599 (2003).
[44]S. J. Plimpton, J. Comput. Phys. **117**, 1 (1995).
[45]C. Bennemann, W. Paul, K. Binder, and B. Dünweg, Phys. Rev. E **57**, 843 (1998).
[46]G. Arya and A. Z. Panagiotopoulos, Macromolecules **38**, 10596 (2005).
[47]A. A. Louis, P. G. Bolhuis, J. P. Hansen, and E. J. Meijer, Phys. Rev. Lett. **85**, 2522 (2000).
[48]J.-P. Hansen and I. R. McDonald, *Theory of Simple Liquids* (Academic Press, Cambridge, 2006).
[49]B. Frick and D. Richter, Science **267**, 1939 (1995).
[50]L. Zhu, X. Wang, Q. Gu, W. Chen, P. Sun, and G. Xue, Macromolecules **46**, 2292 (2013).
[51]C. Friedrichs, S. Emmerling, G. Kircher, R. Graf, and H. W. Spiess, J. Chem. Phys. **138**, 12A503 (2013).
[52]H. Vogel, Phys. Z. **22**, 645 (1921).
[53]G. S. Fulcher, J. Am. Ceram. Soc. **8**, 339 (1925).
[54]G. Tammann and W. Hesse, Z. Anorg. Allg. Chem. **156**, 245 (1926).
[55]C. A. Angell, Science **267**, 1924 (1995).
[56]G. L. Hunter and E. R. Weeks, Rep. Prog. Phys. **75**, 066501 (2012).
[57]B. Frieberg, E. Glynos, and P. F. Green, Phys. Rev. Lett. **108**, 268304 (2012).
[58]A. Chremos, A. Z. Panagiotopoulos, and D. L. Koch, J. Chem. Phys. **136**, 044902 (2012).
[59]F. W. Starr and J. F. Douglas, Phys. Rev. Lett. **106**, 115702 (2011).